Pure Appl. Chem., Vol. 80, No. 9, pp. 1981–1991, 2008.
doi:10.1351/pac200880091981

Modeling time-dependent phenomena in plasma spraying of liquid precursors*

Armelle Vardelle‡, Christophe Chazelas, Cecile Marchand, and Gilles Mariaux

Laboratoire Sciences des Procédés Céramiques et des Traitements de Surface, CNRS University of Limoges, Limoges, France

Abstract: The recently developed plasma spray processes using liquid precursors make it possible to produce finely structured coatings with a broad range of microstructures and, thus, properties. However, coating reproducibility and control of the deposition efficiency are critical to industrial acceptance of these processes. Both depend on time-dependent interactions between the plasma jet and liquid material. Transient and realistic modeling of the liquid spray process may help to increase the understanding of the process. A comprehensive model should involve the formation of the plasma jet inside the torch and the transient specific treatment (break-up, droplet collision, coalescence, evaporation, chemistry) of the liquid material in the plasma jet. If much progress has been recently made on the modeling of the interaction of arc and transverse flow in the plasma torch, further theoretical and experimental research is needed, especially in respect of liquid injection and fragmentation under plasma spray conditions.

Keywords: thermal plasma; plasma spraying; liquid precursor; droplet fragmentation; modeling.

INTRODUCTION

Plasma spraying is now a well-established technology in manufacturing on account of its versatility and cost-efficiency. Plasma coatings are used in original equipment manufacturing but also in repair and maintenance applications. Main uses include aerospace, biomedical, textiles, petrochemicals, mining, and energy production [1]. Therefore, one may think that all the phenomena controlling the plasma spray process have been described and wonder if scientific discoveries can still be made in this technology.

Actually, the phenomena that govern the formation of the plasma jet inside a plasma torch and the formation of coating on the substrate are not completely understood and mastered. Also, the need for performance improvement in industrial systems has sparked a demand for development of coatings with improved physical and mechanical properties. Nanostructured coatings, that is, coatings whose grain sizes are smaller than 100 nm in at least one dimension, have the potential for significant improvement in coating properties, as a decrease in grain size results in a significant increase in the volume fraction of grain boundaries or interfaces [2]. Thus, many research studies in progress relate to the deposition of coatings with a nanoscale microstructure. At present, three methods are mainly employed to elaborate such coatings by plasma spraying. The first one is a two-step process and involves the deposition of

*Paper based on a presentation at the 18th International Symposium on Plasma Chemistry (ISPC-18), 26–31 August 2007, Kyoto, Japan. Other presentations are published in this issue, pp. 1883–2023.

‡Corresponding author

amorphous coatings and their thermal crystallization. This procedure requires material composition with glass-forming ability at plasma spraying cooling rates (~10^6 K/s) and strict control of coating temperature during deposition. It is mostly used for metal alloys, which are readily available in the form of metallic glasses [3].

The second method [4] uses agglomerates of nanoparticles and brings about coatings with a bimodal microstructure formed by semi-molten particles that keep part of the original nanostructure of the powder and fully molten particles that help to maintain coating cohesion. This procedure requires close control of the particle temperatures in the plasma jet to maintain them slightly higher than the melting point of the sprayed material.

Finally, the third route is based on the spraying of liquid feedstock made up of either suspensions of nano- or microsized particles [5–7], or solutions [8,9]. Recent studies [10,11] have shown that liquid feedstock plasma spray techniques can produce either dense or porous coatings depending on process operating conditions and that, when using conventional direct current (DC) plasma torches, they are faced with two main difficulties: (i) the fluctuations of the plasma jet that perturb the injection and penetration of the liquid feedstock into the gas flow and (ii) the property gradients in the plasma jet that result in heterogeneous treatment of the droplets in the core and periphery of the plasma jet. Similar problems are encountered in conventional powder plasma spraying, but in the case of liquid precursors they are aggravated because of the low specific density of droplets that makes them very sensitive to fluctuations of the plasma jet and possible drifts in the nominal conditions of the process. Therefore, in order to develop reliable deposits, fundamental studies are still required to better understand the complex and intertwined interactions between the fluctuating plasma jet and droplets. Models of the process or part of the process can be useful tools in establishing relationships between the process operating conditions and properties of the liquid spray jet, in particular for specific properties that cannot be easily measured, such as the evolution of droplet size and number.

Numerous mathematical models of the *atmospheric plasma spray process* using powders have been proposed in the literature over the last 20 years [12–14]. They have helped to increase the understanding of the process and specific phenomena that cannot be easily measured as heat conduction within the particles, turbulent dispersion of the light particles, and size segregation in the gas flow. They have shown that the entrainment of the cold gas surrounding the plasma jet dominates its behavior as it changes the plasma chemical composition and thus affects the transfer of heat and momentum to injected particles [15]. They have also revealed the importance of the loading effect of the plasma jet by the feedstock material and especially refractory materials [16]. It should be noted that the vaporizing of the powder that in turn will change the thermodynamic and transport properties of the gas and thus the plasma–particle interactions, enhances this effect. In addition, the presence of metal vapors, even at low concentrations, changes the emission power of the plasma gas and, thus, modifies the heat treatment of particles and enhances plasma jet cooling [17].

This paper will discuss the modeling of *time-dependent liquid feedstock plasma spraying* and will concentrate on two specific points that are (i) the modeling of the formation of the plasma jet by the conversion from electrical to thermal energy in the plasma-forming gas and (ii) the interactions of the plasma plume with the droplet jet.

PLASMA JET FORMATION

General remarks

A key aspect of the operation of conventional non-transferred DC plasma torches is the random motion of the arc inside the nozzle. Various plasma gun designs have been developed to limit the arc fluctuations without increasing the heat load to the anode wall, which results in surface erosion and anode wear [18]. However, construction of these plasma torches may be complex while the conventional DC plasma torch mainly consists of a rod-shape cathode and a concentric water-cooled anode and is simple to man-

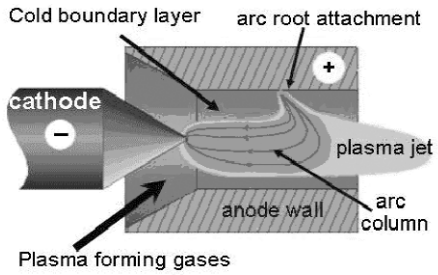

Fig. 1 Schematic representation of a non-transferred DC plasma torch [25].

ufacture and maintain. The arc strikes from the tip of the cathode to some point on the anode wall where it attaches in the form of a high-temperature, low-density gas column cutting through the cold gas boundary layer that covers the anode wall; the thickness of this electrically insulating boundary layer that depends on the torch working parameters (mainly, torch nozzle diameter, arc current intensity, plasma gas nature and flow rate) and the flow conditions control to a great extent the level of fluctuation of the plasma jet issuing from the torch [19,20].

Indeed, the arc attachment perpendicular to the anode surface generally exhibits an axial and rotational movement under the combined action of the drag force exerted by the cold flow in the boundary layer and the Lorentz forces due to the self-magnetic fields induced by the curvature of the current flow [21]. Three arc operation modes have been experimentally observed that differ in the movement of the arc root on the anode wall and the time-evolution of the arc voltage: the steady mode (no distinct motion of arc), takeover mode (more random motion of arc), and re-strike mode (strong fluctuations and steep voltage drops) [15]; mixed modes may also be observed.

The steady mode generally occurs with plasma-forming gases containing diatomic gases like hydrogen and nitrogen, while the takeover mode occurs with monatomic gases like argon and helium.

An accurate description of the arc dynamics is a key component of mastering the liquid feedstock plasma spraying process because of the controlling role that it plays in the plasma flow instabilities, surrounding cold flow entrainment, transition to turbulence, and injection of the liquid material in the plasma flow. The characteristics of the time-variation of the arc voltage (frequency ranging between 1–10 kHz and amplitude variation up to 100 %) are an excellent indication of the level of stability of arc and plasma jet. Thus, their predictions will help to define the processing "window" wherein it is possible to produce, and maintain, a stable droplet spray pattern with consistent trajectories in order to manufacture a coating with a specific microstructure and, also, maximize the deposition efficiency.

Current models

To provide for reasonably good predictive capabilities of plasma torch operation and time-evolution of arc voltage, the model of the arc dynamics must address the 3D and time-dependent interactions between the transverse gas flow and the arc and the nonequilibrium physics involved in the electrode boundary layers. If the phenomena are quite well known, except perhaps the phenomena giving rise to turbulence in this specific medium, the difficulty mostly lies in the ability to understand and compute the consequence of their interplay and especially the way the arc "jumps" from an attachment spot to another or slides on the anode wall. This topic is an active field of research; the 2D and steady models [22,23] have progressed into 3D [24–28] and transient models [29–32]. The latter involve the 3D and transient conservation equations of fluid (mass, momentum, and energy) coupled with the equations of electromagnetism generally written as current conservation and magnetic induction, thanks to the source terms (electromagnetic Lorentz forces in the momentum equation and Joule effect, electromagnetism energy and electron diffusion enthalpy in the energy equation). The electric field and the

magnetic field are determined from the electric potential and the vector potential. Some models also account for the incompressible effects [22,26]. Of course, as in all numerical simulations, the conditions imposed at the boundaries of the domain (plasma-forming gas inlet, plasma flow outlet, cathode and anode walls) and in particular the pressure conditions at the inlet and outlet and, the temperature and current density imposed at the cathode, constrain the predictions. They may differ from one author to another and have to be carefully checked.

Most of the models assume local thermodynamic equilibrium (LTE) in the whole computation domain and require a special treatment of the plasma–electrode interface to allow the passage of current. They generally consider an artificially high electrical conductivity in the anode boundary layer in front of the cathode as the electron temperature is expected to be high near the arc attachment and the electric conductivity of the main plasma-forming gases used in plasma spraying (argon, hydrogen, and nitrogen) is characterized by a critical temperature, about 7000 K, under which it is close to zero.

Two approaches have been used to predict the dynamics of the arc under LTE assumptions: one relies on anode boundary model to account for the dynamics of the arc [24–26] and the other uses an arc reattachment model [23–25,33]. The first approach allows the description of the movement of the anode attachment on the anode wall and formation of a new attachment when the arc gets close to the anode surface. This approach, which has been commonly used in steady-state simulations of thermal plasmas [19–21], enables us to describe the steady and takeover modes of arc operation.

The second approach makes it possible to describe the restrike mode by mimicking the physical process by which a new arc attachment is formed in a region upstream of the original attachment when the available voltage in the arc is larger than the breakdown voltage. A Boolean, based on the value of "a critical electric field, E_b", allows us to define the location of the gas breakdown while the arc root reattachment process is obtained by introducing either a high-temperature or high electrical conductivity channel between the arc and anode surface. At the moment, reattachment models can be tuned to match either the experimentally measured peak frequency or the total voltage drop, but not both simultaneously.

Recently, a nonequilibrium model has been proposed by Trelles et al. [33] under takeover arc mode condition (argon plasma gas) that takes into account the temperature of the electrons and heavy species and involves four species for argon gas, assuming chemical equilibrium. This model can be considered as the most accomplished at the moment. The total voltage drops of the nonequilibrium results are still slightly higher than those measured, but the overall shape of the voltage signal resembles that measured experimentally, indicating the takeover mode of operation of the torch. However, as written by the authors, nonequilibrium simulations of the restrike operation mode will still need a breakdown model to produce more realistic results.

Some examples of results under arc restrike mode conditions

The results, drawn from refs. [23,25], concern a plasma spray torch that uses as inlet gas a mixture of argon and hydrogen injected with a swirl movement in the arc chamber of the torch. The operating conditions combine a high gas flow rate (60 slm) and hydrogen content (25 %) so that the actual arc operated in the breakdown-restriking mode when the arc current was varied between 300–600 A and the nozzle internal diameter between 6–7 mm [14].

Figure 2 shows that the arc voltage presents a saw-tooth evolution, characteristic of the restrike mode operation for the arc. The variations in the length and width of the arc column in the anode nozzle give rise to the time variation of the maximum gas temperature and velocity at the exit nozzle, as illustrated in Fig. 3 for the flow velocity. These fluctuations are in unison with the voltage fluctuation that reflects the variation in arc column length. The predictions show that an increase in the arc current intensity results in both a decrease of the voltage jump amplitude and an increase of the restrike frequency as experimentally observed [14]. They also show that, as expected, an increase in arc current (Fig. 4) brings about an increase in the gas velocity and specific enthalpy at nozzle exit (Figs. 4 and 5, respec-

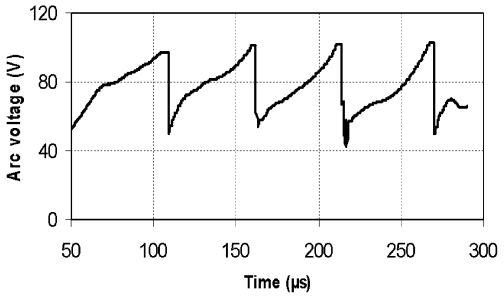

Fig. 2 Predicted time-evolution of the arc voltage. $D_{\text{nozzle i.d.}}$= 7 mm; I = 300 A, 45 Nl/min Ar +15 Nl/min/ H_2.

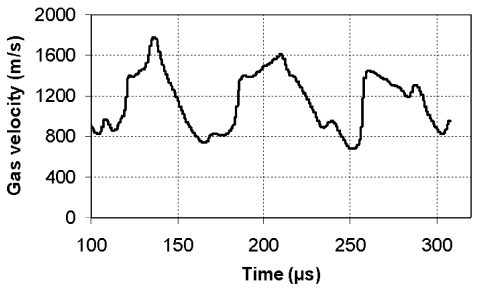

Fig. 3 Predicted time-evolution of gas velocity at the torch exit on torch axis. $D_{\text{nozzle i.d.}}$= 7 mm; I = 300 A.

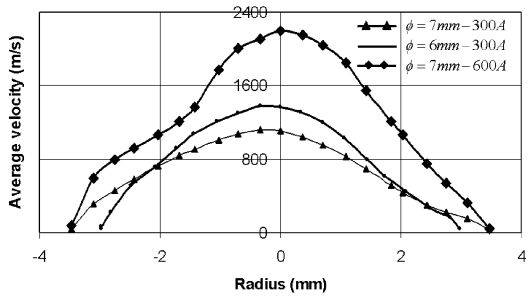

Fig. 4 Predicted time-averaged radial profile of gas velocity at nozzle exit; $D_{\text{nozzle i.d.}}$= 7 mm; I = 300 A, 45 Nl/min Ar +15 Nl/min/ H_2.

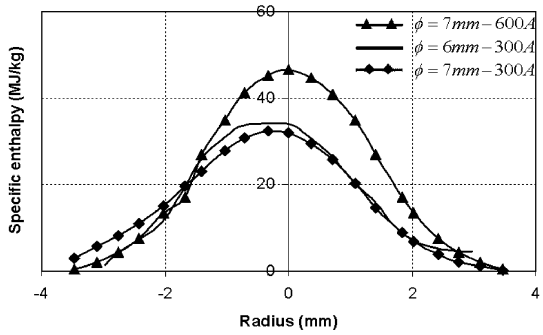

Fig. 5 Predicted time-averaged radial profile of gas specific enthalpy at nozzle exit.

tively). The mean value of gas velocity on the torch axis passes from 1300 to 2000 m/s while the variations in gas temperature are slightly noticeable as between 9000–20 000 K, the heat is stored in the gas species in the form of ionization energy that acts as a thermal inertia wheel and dampens the plasma temperature variation.

LIQUID FEEDSTOCK INJECTION AND BEHAVIOR IN THE FLOW

Liquid injection

With conventional DC plasma torches, the liquid feedstock is generally injected transversally into the plasma jet by pneumatic (use of an atomization gas that may perturb the plasma flow) or mechanical injection in the form of a droplet spray (5–300 μm in diameter) or a liquid jet. The latter may have kept an intact liquid core up to the moment it hits the plasma flow or, most likely, have undergone a primary break-up and, thus, consists of discrete blobs of liquid. Irrespective of the injection system, the behavior of the droplets or liquid stream in the plasma will depend on the instant when they are injected in the flow and, of course, level of fluctuation of the plasma flow. Indeed, as in conventional powder plasma spraying, the injection of the liquid material in the plasma flow is controlled by the instantaneous momentum flux of the plasma jet $\rho_{gas}.v^2$ (transport rate of momentum per unit cross-sectional area) compared to its own momentum flux $\rho_l.v^2$ and by the viscosity of the gas at the location of injection.

Figure 6, drawn from ref. [35], shows an argon–hydrogen plasma jet (5000-K isotherm colored by the mass fraction of plasma gas) at various instants of the arc fluctuation period and the corresponding gas momentum flux in the liquid feedstock injection plane. These predictions result from a 3D and time-dependent model of the plasma jet issuing in air in conjunction with a large eddy simulation (LES) turbulence model [36]. As the droplet momentum imparted by the carrier gas cannot follow the arc root fluctuations, the droplet trajectories are expected to fluctuate accordingly and also the acceleration and treatment of the droplets.

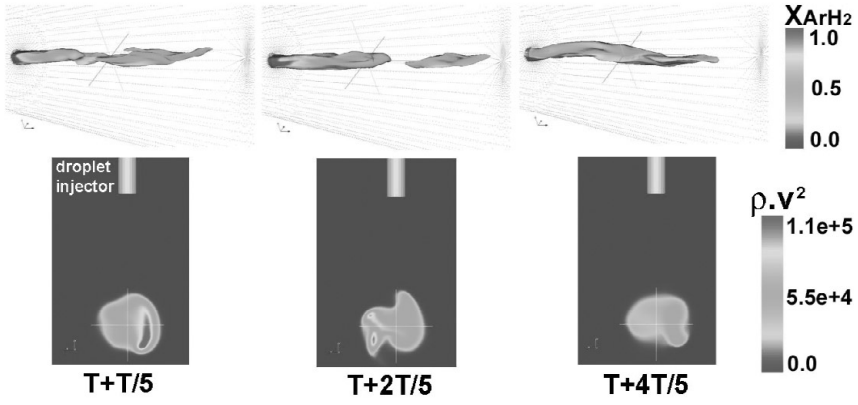

Fig. 6 Time-evolution of the 5000-K isotherm colored by the mass fraction of plasma gas and of the gas momentum density ($kg \cdot m^{-1} \cdot s^{-2}$) in the droplet injection plane. *T* is the arc fluctuation period. Ar (45 NL/min); H_2 (15 NL/min); arc current: 600 A; torch nozzle diameter: 6 mm .

These figures corroborate the experimental observation that the injection stage is a very delicate stage of the process because of the low density of the liquid feedstock and eventual break-up of the liquid material that makes its penetration trickier. Therefore, a possible ideal movement for the arc attachment would be a quasi-periodic movement with high arc fluctuation frequency and low amplitude variation. This arc mode will help both to spread the thermal load of the arc attachment over the anode

wall and, so, limit the anode wear, and achieve a quasi-stable plasma. It has been shown experimentally that such fluctuation conditions can be approached by using mono-atomic gases (e.g., mixture of helium and argon) and appropriately choosing the torch geometry, gas mass flow rate, and arc current [37].

Now, when the liquid stream or droplets penetrate the plasma jet, they exhibit a rather different behavior of solid particles, as they will undergo both fragmentation and evaporation and eventually counteracting collisions and coalescence in the zones where the liquid loading is high enough. During the injection phases, the liquid break-up is mainly due to mechanical phenomena, while further downstream, thermal fragmentation due to the internal boiling of the liquid may also affect the liquid dispersion in the plasma jet.

A comprehensive model of the liquid feedstock plasma spray process should involve (i) the formation of the primary plasma jet inside the plasma torch; (ii) discharge of the transient plasma jet in the surrounding gas; (iii) mechanical, thermal, and, eventually, chemical interactions between the droplets and plasma jet and between the droplets themselves (collision, coalescence); and (iv) material impact on the substrate. It should be noted that if the suspension and solution droplets are subjected to the same mechanical fragmentation processes, their treatment in the plasma flow will differ: Once the solvent is evaporated, the fine particles contained in the suspension droplets are heated and accelerated and impact, in a molten or semi-molten state, on the substrate, depending on the particle trajectories as in conventional plasma spraying. In the case of solution, the precursor undergoes evaporation followed by precipitation, pyrolysis, sintering, melting, and eventually crystallization; the last two mechanisms occurring essentially for longer stand-off distances. In fact, depending on their trajectory, the droplets will experience the whole or a part of these mechanisms [38,39].

A complete model of the process is still a challenge and requires the independent (as far as possible) study and validation of the various subprocesses that govern the plasma flow and droplets. A key point of the model, which has not been much investigated yet in plasma spray conditions, is the ability of the model to predict the droplet fragmentation, as this mechanism will condition the trajectories of droplets and their subsequent treatment in the plasma flow. Calculations of droplet fragmentation by using a force balance between the drag force and surface tension force showed that the fragmentation time of droplets 50–300 μm in diameter is shorter by 2 to 3 orders of magnitude than their vaporization time [40], and, thus, they strengthen the assertion that this mechanism is one of the most important to investigate to understand the process.

In this paper, we will limit our discussion to this topic and consider only the secondary break-up of droplets, which is droplet fragmentation into ever smaller droplets, as most of the injection devices deliver droplets or blobs.

Droplet break-up

A vast literature deals with droplet break-up mechanisms as atomization plays an important role in a wide variety of technical applications, e.g., coating applications, gas turbines and diesel engines, inkjet printers, etc. (see, e.g., the course of Reitz at <http://www.erc.wisc.edu/modeling/spray_course/>). However, these mechanisms are still not completely understood for high-velocity and, even more, high-temperature conditions that will speed up the vaporization process.

The droplet break-up regimes are generally categorized according to the dimensionless Weber number that expresses the ratio of inertia forces to surface tension forces ($We = \rho_{gas} u_r^2 D_{drop}/\sigma_l$). They can be classified as bag ($12 < We < 100$; deformation of the drop as a bag-like structure that is stretched and swept off in the flow direction), stripping ($12 < We < 100$; thin sheets are drawn from the periphery of the deforming droplets), and catastrophic regime ($We > 350$; multistage breaking process) according to increasing the Weber number [41].

Droplet break-up can be described either by empirical correlations [31,42,43] or mathematical models. The latter make it possible to predict the distortion and aerodynamic break-up of the droplet

as the popular wave model of Reitz et al. [44] or the Taylor analogy break-up (TAB) of O'Rourke et al. [45]. The wave model supposes that the break-up time and the resulting droplet size are related to the fastest growing Kelvin–Helmholtz (K–H) instability*, while the TAB model is based on the analogy between a spring mass system and an oscillating and distorting droplet; it describes via a linear equation, the deformation of the droplet under a forcing (aerodynamic droplet–gas interaction), restoring (surface tension), and damping (liquid viscosity) terms and predicts the size of the daughter droplets by equating the energy of the parent drop to the combined energy of the daughter droplets. The wave model is better used for larger Weber numbers as the TAB model does not describe well the stripping break-up.

In liquid precursor plasma spraying, it may be expected that the drops experience different break-up regimes because of the steep radial gradient of plasma flow properties and time-variation of these properties. They will depend on droplet size, injection velocity, and plasma flow characteristics at the instant they penetrate the gas flow, especially at the liquid injection location. Experimental data carefully established under controlled spraying conditions are, thus, essential for better understanding the behavior of the droplets in the gas flow and validating the models. Some recent experimental observations of the liquid material in the plasma jet can be found in the literature [31,46,47]. They use laser pulses to visualize the droplets in the bright plasma medium.

Figure 7 shows [47] photographs of 250-μm-diameter water drops deflected and broken up when penetrating the plasma jet.

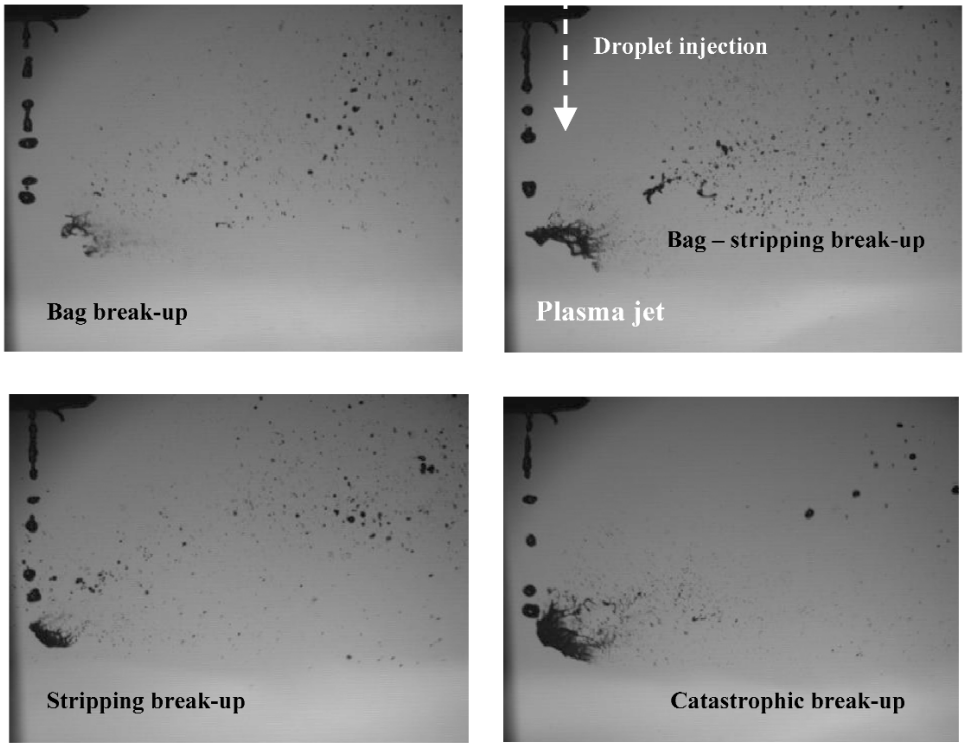

Fig. 7 Photographs of 250-μm-diameter water drops penetrating the transverse plasma jet. Various break-up regimes are observed depending on the time when the drops penetrate the gas flow. Torch nozzle exit diameter: 7 mm; arc current: 600 A; gas flow rate: 45 Nl/min Ar +15 Nl/min H_2.

*K–H instability is caused by the viscous forces due to the relative motion of the two phases at the phase-dividing interface.

Under plasma spray conditions, it seems interesting to use a model that may account for the various break-up regimes as the enhanced TAB (ETAB) model proposed by Tanner [48]. This model uses the droplet deformation dynamics of the TAB model but describes the droplet break-up thanks to an exponential law which links the mean daughter droplet size to the break-up time of the parent drop. The main assumption for the droplet break-up is that the rate of daughter droplet generation, $dn(t)/dt$, is proportional to the number of the product droplets $n(t)$ as follows: $dn(t)/dt = -3\ K\ n(t)$ where the proportionality constant, K, depends on the break-up regime: $K = k_1\omega$ if $We \leq We_t$ and $K = k_2\omega(We)^{1/2}$ if $We > We_t$. We_t is a regime-dividing Weber number and may be set to 160 and $\omega = [8\sigma_l/(\rho_l.R^3_{drop})]^{1/2}$ is the pulsation of the droplet instability. Thus, the number of product droplet is linked to the breaking time via the following equation: $n(t) = \exp(3Kt_{br})$ where k_{br} is the break-up time. Also, the average mass, and average size of the daughter droplets is determined from $m_{ave}(t) = m_0/n(t)$ where m_0 is the mass of the parent droplet and $n(t)$ the number of product droplets. An energy balance between the parent and daughter drops brings about an expression for the product droplet velocity component normal to their trajectory.

It should be noted that droplet break-up models generally include parameters and constants that are generally determined from theoretical considerations and experimental results. For example, k_1 and k_2 constants in the Tanner's model have been determined to match the drop sizes and velocities experimentally determined by Schneider [49] for Diesel sprays and set to $k_1 \sim k_2 = 1/4.5$.

Some of these models are implemented in commercial computational fluid dynamics (CFD) codes, but their constants still need to be validated for plasma spraying conditions [39,50]. However, experimental studies are still scarce and subject to uncertainties that make them difficult to use for model validation. As a matter of fact, the latter requires the quantification of the number and size of droplets in the plasma flow. However, the zone of injection where the liquid material is dense is difficult to analyze. Further downstream, the liquid jet is less dense but the droplets that have undergone fragmentation and vaporization are also not easy to detect under plasma conditions and, moreover, they do not provide a direct test of injection modeling because of the possible variation in size and numbers.

CONCLUSION

The development of the plasma spray processes using a liquid feedstock makes essential the control of the time-dependent phenomena, which govern to a large extent the quality and reproducibility of the product and lead to intensive research in various laboratories. The modeling of the process proves to be a basic tool to understand these phenomena and contribute to their control. A comprehensive model of the process should involve the formation of the primary plasma jet inside the plasma torch and its discharge in the surrounding gas coupled with the injection and treatment of the liquid material in the jet. Much progress has been recently made on the modeling of the arc dynamics inside the plasma torch and the interaction of the arc with the transverse gas flow. However, the specific treatment of the liquid material in the plasma flow that involves fragmentation, eventual collision and coalescence of the subsequent droplets, evaporation, and some chemistry, requires the development of dedicated models or adaptation of the models that have been established for sprays under conditions different from plasma spray conditions. This suggests a definite need for experimental data that have been carefully established under controlled spraying conditions in order to validate the models of droplet treatment.

REFERENCES

1. J. R. Davis. *Handbook of Thermal Spray Technology*, ASM International, Materials Park, OH (2004).
2. *Handbook on Nanoscience, Engineering and Technology*, 2nd ed., Taylor & Francis (2007).
3. D. Branagan, A. V. Sergueeva, A. K. Mukherjee. *Adv. Eng. Mater.* **8**, 940 (2006).
4. R. S. Lima, B. R. Marple. *J. Therm. Spray Technol.* **16**, 40 (2007).

5. P. Fauchais, V. Rat, C. Delbos, J. F. Coudert, Th. Chartier, L. Bianchi. *IEEE Trans. Plasma Sci.* **33**, 920 (2005).
6. B. Philip, K. Seiji. *J. Am. Ceram. Soc*. **84**, 1257 (2001).
7. J. Berghaus-Oberste, B. Marple. *J. Therm. Spray Technol.* **15**, 676 (2006).
8. J. Karthikeyan, C. C. Berndt, S. Reddy, J. Wang, A. H. King, H. Herman. *J. Am. Ceram. Soc.* **81**, 121 (1998).
9. N. P. Padture, K. W. Schlichting, T. Bhatia, A. Ozturk, B. Cetegen, E. H. Jordan, M. Gell, S. Jiang, T. D. Xiao, P. R. Strutt, E. Garcia, P. Miranzo, M. I. Osendi. *Acta Mater.* **49**, 2251 (2001).
10. P. Fauchais, G. Montavon, M. Vardelle, J. Cedelle. *Surf. Coat. Technol.* **201**, 1908 (2006).
11. A. Jadhav, N. Padture, F. Wu, E. Jordan, M. Gell. *Mater. Sci. Eng. A* **405**, 313 (2005).
12. A. Vardelle, P. Fauchais, M. Vardelle, G. Mariaux. *Adv. Eng. Mater*. **8**, 599 (2006).
13. I. Ahmed, T. L. Bergman. *J. Therm. Spray Technol.* **9**, 215 (2000).
14. B. Liu, T. Zhang, D. T. Gawne. *Surf. Coat. Technol.* **132**, 202 (2000).
15. E. Pfender, J. Fincke, R. Spores. *Plasma Chem. Plasma Process.* **11**, 529 (1991).
16. R. Ye, P. Proulx, M. Boulos. *J. Phys. D: Appl. Phys.* 33. 2154 (2000).
17. A. Essoltani, P. Proulx, M. I. Boulos, A. Gleizes. *Plasma Chem. Plasma Process*. **14**, 437 (1994).
18. M. Dzulko, G. Forster, K. B. Landes, K. Nassenstein. *Proc. International Thermal Spray Conference*, E. Lugscheider (Ed.), 2–4 March 2005, Basel, Switzerland, DVS Deutscher Verband für Schweißen (2005).
19. R. Hartmann, J. Heberlein. *J. Phys. D: Appl. Phys*. **34**, 2972 (2001).
20. C. Chazelas, J. F. Coudert, P. Fauchais. *IEEE Trans. Plasma Sci.* **33**, 416 (2005).
21. J. Heberlein. *High Temp. Mater. Process*. **6**, 321 (2002).
22. O. H. Chang, A. Kaminska, M. Dudeck. *J. Phys. III* **7**, 1361 (1997).
23. J.-M. Bauchire, J.-J. Gonzalez, A. Gleizes. *J. Phys. III* **7**, 829 (1997).
24. A. Kaddani, S. Zahrai, C. Delalondre, O. Simonin. *J. Phys. D: Appl. Phys.* **28**, 2294 (1995).
25. H.-P. Li, X. Chen. *J. Phys. D: Appl. Phys.* **34**, L99 (2001).
26. J. J. Gonzales, P. Freton, A. Gleizes. *J. Phys. D: Appl. Phys.* **35**, 3181 (2002).
27. H.-P. Li, X. Chen, E. Pfender. *J. Phys. D: Appl. Phys.* **36**, 1084 (2003).
28. L. Klinger, J. B. Vos, K. Appert. *Preprint Report*, *LRP 763*, <http://crppwww.epfl.ch/> (2003).
29. C. Baudry, A. Vardelle, G. Mariaux. *High Temp. Mater. Process.* **9**, 1 (2005).
30. V. Colombo, E. Ghedini. *Proc. 17th Int. Symp. Plasma Chemistry*, Toronto, Canada, p. 169 (2005).
31. E. Moreau, C. Chazelas, G. Mariaux, A. Vardelle. *J. Therm. Spray Technol.* **15**, 524 (2006).
32. J. P. Trelles, E. Pfender, J. V. R. Heberlein. *Plasma Chem. Plasma Process.* **26**, 557 (2006).
33. J. P. Trelles, E. Pfender, J. V. R. Heberlein. *J. Phys. D: Appl. Phys*. 40, 5635 (2007).
34. J. P. Trelles, J. V. R. Heberlein, E. Pfender. *J. Phys. D: Appl. Phys*. **40**, 5937 (2007).
35. C. Marchand, C. Chazelas, G. Mariaux, A. Vardelle. *J. Therm. Spray Technol.* **16**, 705 (2007).
36. P. Sagaut. In *Mathématiques et Applications*, Springer Verlag **30** (1998).
37. R. Etchart-Salas, V. Rat, J. F. Coudert, P. Fauchais, N. Caron, K. Wittman, S. Alexandre. *J. Therm. Spray Technol.* **16**, 857 (2007).
38. L. Xie, X. Ma, A. Ozturk, E. H. Jordan, N. P. Padture, B. Cetegen, D. T. Xiao, M. Gell. *Surf. Coat. Technol.* **183**, 51 (2004).
39. S. Basu, E. Jordan, B. Cetegen. *J. Therm. Spray Technol*. **1**, 60 (2007).
40. C. Delbos. *Understanding the Injection of Metal or Ceramics Suspensions in a DC plasma jet,* Ph.D. Thesis, in French, University of Limoges, France <http://www.unilim.fr/theses/2004/sciences/2004limo0035/html/index-frames.html> (2004).
41. M. Pilch, C. Erdmann. *Int. J. Multiphase Flow* **13**, 741 (1987).
42. R. D. Reitz, R. Diwakar. *SAE Technical Paper* 860469 (1986).
43. L.-P. Hsiang, G. M. Faeth. *Int. J. Multiphase Flow* **18**, 635 (1992).
44. R. D. Reitz. *Atom. Spray Technol.* **3**, 309 (1987).

45. P. J. O'Rourke, A. A. Amsden. *SAE Technical Paper* 872089 (1987).
46. J. Oberste-Berghaus, J. G. Legoux, C. Moreau. *Proc. Int. Thermal Spray Conference*, E. Lugscheider (Ed.), 2–4 March 2005, Basel, Switzerland, DVS Deutscher Verband für Schweißen (2005).
47. A. Vardelle, C. Marchand, G. Mariaux, P. Lefort. *Surf. Coat. Technol.* **202**, 4458 (2008).
48. F. X. Tanner. *SAE Technical Paper* 970050 (1997).
49. B. Schneider. Experimental investigation of diesel sprays. CRFD and Laser Diagnostic Workshop, *21#l CIMAC Congress 1995,* Interlaken, 16 May 1995.
50. Y. Shan, T. W. Coyle, J. Mostaghimi. *J. Therm. Spray Technol.* **16**, 698 (2007).